

CREEP FATIGUE CRACK GROWTH OF SEMI-ELLIPTICAL DEFECT IN
AUSTENITIC STAINLESS STEEL PLATES

F. CURTIT[♦], L. LAIARINANDRASANA[∇], B. DRUBAY[♦] and B. MARTELET[⊕]

In this paper, a creep-fatigue crack growth test performed on a large austenitic stainless steel plates containing a $\frac{1}{2}$ elliptical Centred Notch under Bending (SCNB specimen) is presented. The experimental crack growth data is simulated using global fracture mechanics parameters including ΔK and C^* issued from the reference stress approach for the determination of the respective fatigue and creep growth rates. The methods are presented in details and the choice of the reference stress for the calculation of the global parameters is examined. It is found that the methods provide predictions in good agreement with the experimental data.

INTRODUCTION

The purpose of the work reported here is to perform experiments on large cracked specimens in order to propose and validate new methods for defect assessments of industrial components operating at high temperatures. Within this scope, the PLAQFLU program, resulting from a collaboration between CEA, EDF and FRAMATOME in France, has for main objective to propose creep-fatigue crack propagation models for semi-elliptical defects in 316L(N) stainless steel plates at 650°C. In a first section, an outline of the creep-fatigue experiment is given. In this test, over 3000 creep-fatigue cycles were applied to the specimen and substantial crack growth was observed, both through the thickness and on the surface of the plate. In a second section, the model used for the simulation together with the needed material properties are presented. This model is based on a linear summation of the fatigue and creep crack growth rates contributions, estimated from global fracture mechanics quantities such as ΔK and C^* . Two different expressions of the reference stress are used with this model accounting differently for the influence of the crack geometry. The simulated results compare favourably well with the experimental data.

♦ CEA, DRN/DMT/SEMT/LISN, Gif-sur-Yvette Cedex, F-91191.

∇ Centre des matériaux ENSMP, UMR CNRS 7633

⊕ EDF SEPTEN, Villeurbanne Cedex, F-69628.

TESTING FACILITY AND EXPERIMENTAL PROCEDURE

The specimen consists of a 316L(N) stainless steel plate containing a ½ elliptical Centred Notch under Bending (SCNB). The SCNB specimen is subjected to cyclic bending loads with a one hour holdtime at the maximum load. The bending load is imposed using two 150 mm long grips bolted to the ends of the plate 1.

The test is carried out at a nominal temperature of 650°C and the furnace is adjusted so that the thermal gradient across the width of the plate and over a length of 190mm remains less than ±2.5°C. A number of parameters are recorded during the test, including the load and displacement applied to the plate, the rotation angle of the grips and the relative plate deflection with respect to the furnace. These measurements allow to determine the effective bending moment applied to the specimen. In addition, crack growth is monitored using a pulsed potential drop technique. Additional information concerning this type of experiment has been reported elsewhere (1).

The loading cycle consists of a trapezoidal waveform under imposed load conditions at a load ratio R=0.1 with a one hour holdtime (T_h) at the maximum load of the cycle. High temperature fatigue pre-cracking is first performed in order to obtain a sharp crack from the machined notch. Two beachmarks of the crack surface were also made with a pure fatigue loading cycle in order to obtain intermediate crack fronts. The resulting crack surface obtained at the end of the test is shown in figure 1 and the crack dimensions are summarised in table 1 as a function of the number of cycles.

ANALYSIS

The creep fatigue crack growth analysis presented in this paper is based upon defect assessment methods described in the French A16 document (2). The model deals with the fracture mechanics quantities ΔK and C*_s(t) that are estimated from the reference stress approach. In this simulation, the geometry of the defect is considered as a ½ ellipse for which axes correspond to the through thickness (a) and surface (2c) crack dimensions, respectively. The crack growth process is modelled through the thickness and on the surface of the plate using a linear summation of both fatigue and creep crack growth rates contributions. The total crack growth rate per cycle da/dN is given by :

$$\frac{da}{dN} = \left(\frac{da}{dN} \right)_{fat} + \left(\frac{da}{dN} \right)_{creep} \quad (1)$$

The crack dimensions are updated after each cycle. The fatigue contribution is calculated using the Paris law of the material given in table 2. This Paris law is obtained from a similar specimen subjected to continuous fatigue loading conditions. The effective Stress Intensity Factor (SIF) range is given by (2) :

$$\Delta K_{eff}(a,c) = \Delta K_{RN}(a,c) \cdot \sqrt{\frac{E^* \cdot \Delta \epsilon_{ref}}{\Delta \sigma_{ref}} + \frac{0.5 \Delta \sigma_{ref}^2}{\Delta \sigma_{ref}^2 + 4 \cdot \sigma_y^2}} \quad (2)$$

In Eqn. 2, the SIF range $\Delta K_{RN(a,c)}$ is calculated using the Raju and Newman stress intensity factor formulae. The correction applied to ΔK_{RN} proposed in the A16 document (2) allows to account for plasticity. $\Delta\sigma_{ref}$ is the reference stress range and $\Delta\varepsilon_{ref}$ the corresponding reference strain range calculated using the cyclic curve of the material. For the simulation, the expression and parameters of the cyclic curve and the yield stress of the material σ_y are given in table 2. They are both taken from the RCC-MR document. The stress state is modelled assuming $E^*=E$ for plane stress conditions on the surface point and $E^*=E/(1-\nu^2)$ for plane strain conditions at the deepest point of the crack.

The creep contribution is obtained by continuous integration of the creep crack growth law during the holdtime of each cycle. Creep is not reinitiated at the beginning of the holdtime. This model has been first developed for CT specimens (4) and successfully used for plates containing $\frac{1}{2}$ elliptical cracks (1). For the calculation, the creep crack growth law (table 1) was identified on CT specimens and is reported in (4). The integration of the creep crack growth propagation law reduces to :

$$\left(\frac{da}{dN}\right)_{creep} = \int_t^{t+T_h} A.(C_s^*(t))^q .dt \text{ or } \left(\frac{da}{dN}\right)_{creep} = \int_N^{N+1} A.(C_s^*(t))^q .T_h .dN \quad (3)$$

where $C_s^*(t)$ is estimated using the expression proposed in the A16 document :

$$C_s^*(t) = \left(\frac{K_{RJ}^2}{E^*}\right) \cdot \frac{\dot{\varepsilon}_{ref}(t).E}{\sigma_{ref}} \quad (4)$$

$\dot{\varepsilon}_{ref}(t)$, corresponding to the reference stress σ_{ref} , is the creep reference strain rate estimated using the creep law of the material. In the model, the creep laws of the material were identified from uniaxial creep tests at different load levels (table 1). Two different reference stress expressions are employed for the calculations and both of them assume that the membrane stress is negligible in comparison with the bending stress. The first one, proposed in the A16 document (2), can be expressed for a pure bending load by :

$$\sigma_{ref} = \frac{2}{3} |\sigma_b| = \frac{2}{3} \left| \frac{6.B.L}{2.b.h^2} \right| \quad (5)$$

where L is the maximum load applied to the plate and B the length of the bending arm. Eqn. 5 results from a limit load analysis of a plate where the influence of the defect is neglected. In Eqn. 2, $\Delta\sigma_{ref}$ is obtained from Eqn. 5 by replacing the maximum load L with the load range ΔL .

The second expression of the reference stress is obtained from a limit load analysis that accounts for the influence of the defect geometry on the limit bending moment M_L . For such a geometry and loading conditions, the membrane stress is assumed to be negligible in comparison to the bending stress. The considered limit load is that obtained for a cracked plate subjected to pure bending loads :

$$M_L = 2 \cdot \sigma_y \cdot \left(\int_0^c \frac{1}{2} \left(h - a \cdot \sqrt{1 - \left(\frac{y}{c} \right)^2} \right)^2 \cdot dy + (b - c) \cdot \left(\frac{h}{2} \right)^2 \right) \quad (6)$$

and the reference stress is given by :

$$\sigma_{ref} = \frac{M_{max} \cdot \sigma_y}{M_L} = \frac{2}{3} \cdot \frac{\sigma_b}{1 + \frac{a}{h} \cdot \frac{c}{b} \cdot \left(\frac{2}{3} \cdot \frac{a}{h} - \frac{\pi}{2} \right)} \quad (7)$$

In order to model correctly the experiment, it is necessary to account for the plate deflection that decreases continuously during the test and reduces the effective length of the bending arms. This is achieved using a 4th order polynomial fitted to the distribution of the bending arm length as a function of crack depth measured during the experiment.

DISCUSSION

The predictions obtained with the model are compared with the experimental data in figures 5 and 6 for the depth and surface crack growth, respectively. Using the reference stress solution proposed in the A16 document (Eqn. 5), the predicted crack depth corresponding to the end of the test is approximately 1.4 times higher than the one observed experimentally. On the surface, this conservatism reduces to a factor of 1.3. When using the second reference stress accounting for the crack dimensions on the expression of the limit bending load (Eqn. 6), this conservatism increases to a factor of 1.65 through the thickness and a factor of 1.5 on the surface. The model is found to produce reasonably conservative predictions in agreement with the experimental data.

The reference stress solution proposed in the A16 document provides better results than the proposed reference stress that is supposed to better describe the specimen behaviour. In the meantime, this work is still going on. Further investigations are required concerning :

- The material properties : It is expected that the identification of the creep crack growth law obtained specifically for the material constituting the plate will decrease the conservatism.
- The way to account for the shape of the crack, which does not correspond exactly to a ½ elliptical shape.
- The estimation of fracture mechanics parameters (the simplified methods used probably overestimates the values of ΔK_{eff} and C* parameters).
- The crack growth model (linear summation of creep and fatigue crack growth rates).

CONCLUSIONS

In this paper, the behaviour of an austenitic stainless steel plate containing ½-elliptical Centred Notch under Bending, subjected to creep-fatigue crack growth test has been analysed. The results have been presented and the following conclusions can be made :

- The trend of the creep-fatigue crack growth experimental data is well described by the simulation.
- A reference stress that is expected to better approximate the mechanical behaviour of the specimen has been proposed.

Further work is needed to improve the simulation. This includes the identification of a creep crack growth law specific for the material constituting the plate and a stress intensity factor solution that better describes the geometry of the crack shape.

REFERENCES

- (1) C. Poussard & al, 1998, *Creep-Fatigue Crack Growth in Austenitic Stainless Steel Centre Cracked Plates at 650°C - Part I & II*, Proceedings of SISSI 3 / HIDA, S3-22 (Part I), S7-48 (Part II), Saclay, FRANCE.
- (2) B. Drubay, "A16 : guide pour l'analyse de la nocivité de défauts et la fuite avant rupture", 3ème version préliminaire, rapport DMT 95.659 du 12.95.
- (3) J.C. Newman, & I.S. Raju, 1981, *An Empirical Stress Intensity Factor Equation for Surface Cracks*, Engineering Fracture Mechanics, 15/1 and 2, 185-192.
- (4) J.P. Polvora, B. Drubay, R. Piques and B. Martelet, 1997, *Creep-Fatigue Crack Growth in on CT25 Specimens in an 316L(N) Austenitic Stainless Steel at 650°C*, SMIRT 14, Division G, paper 322, 17-22/08, Lyon, FRANCE.

| Material properties | Expression | Parameters value |
|---|--|---|
| Young modulus | E (MPa) | 140600 |
| Yield stress | σ_y (MPa) | 125 |
| Cyclic curve | $\Delta\varepsilon = 100 \cdot \frac{\Delta\sigma}{E} + \left(\frac{\Delta\sigma}{k}\right)^{\frac{1}{m}}$ $\Delta\varepsilon$ (mm/mm) | k=678 m=0.239 |
| Uniaxial primary and secondary creep laws | $\varepsilon_p = B_1 \cdot \sigma^{n_1} \cdot t^{p_1} \quad \text{for } t < t_{ffp}$ $\varepsilon_p = B_1 \cdot \sigma^{n_1} \cdot t_{ffp}^{p_1} + B_2 \cdot \sigma^{n_2} \cdot (t - t_{ffp})^{n_2} \quad \text{for } t > t_{ffp}$ $\text{with : } t_{ffp} = \left(\frac{B_2}{B_1 \cdot p_1} \cdot \sigma^{n_2 - n_1}\right)^{\frac{1}{p_1 - 1}} t(h)$ | $p_1 = 0.565$ $B_1 = 5.013 \cdot 10^{-12}$ $n_1 = 3.878$ $B_2 = 5.532 \cdot 10^{-24}$ $n_2 = 8.767$ |
| Paris law | $\frac{da}{dN} = C \cdot \Delta K^n \frac{da}{dN}$ (mm / mm) ; ΔK (MPa \sqrt{m}) | C = 6.074 10 ⁻⁸ n = 2.808 |
| Creep crack growth law | $\frac{da}{dt} = A \cdot (C^*)^q \frac{da}{dt}$ (mm / h) ; C*(N / mm.h) | A = 0.007 q = 0.73 |

Table 1 : Material properties at 650°C used for the simulation

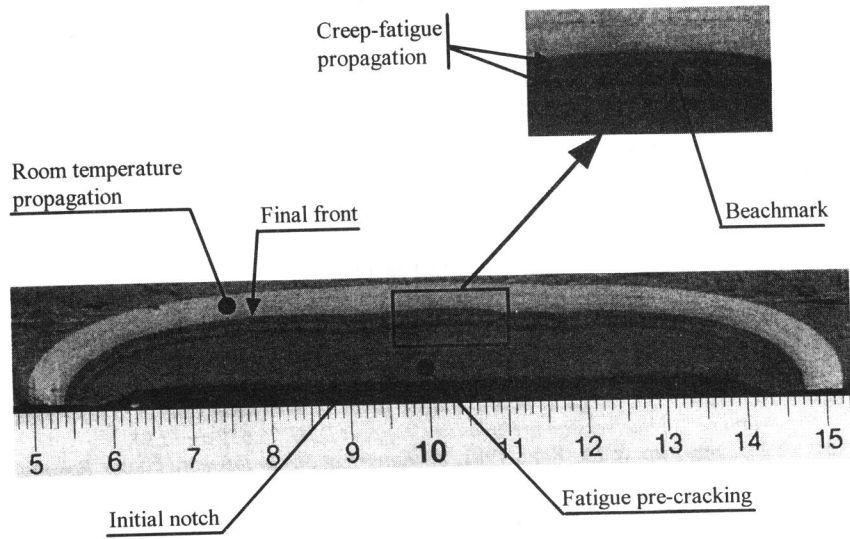


Figure 1 : Crack surface of the SCNB specimen

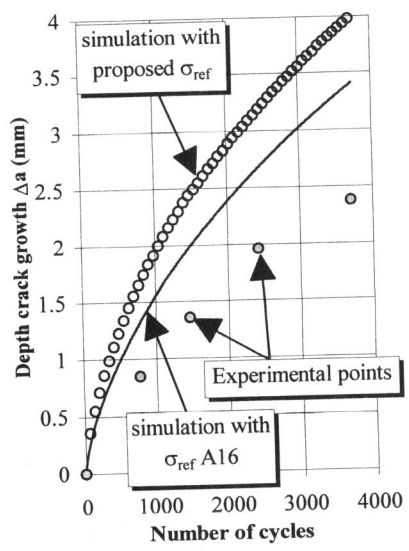


Figure 2 : Depth crack growth versus number of cycles

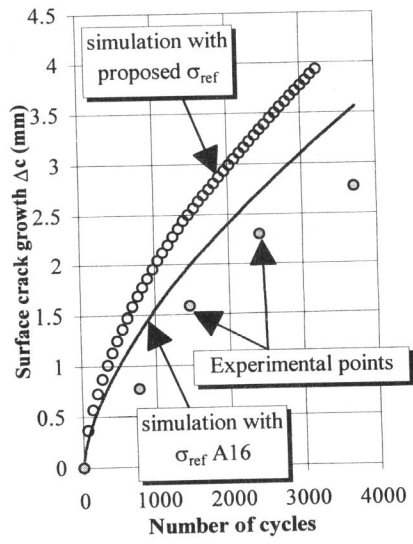


Figure 3 : Surface crack growth versus number of cycles